Nanotechnology Perceptions
ISSN 1660-6795
www.nano-ntp.com

Development of Attention Guided Hybrid Network with Adaptive FCM-aided Segmentation for Predicting the Liver Disease

A.Venu Madhavi[1], Srinivas Prasad[2*]

[1]*Research Scholar, Department of Computer Science and Engineering, Gitam University, Visakhapatnam, India, vaedodod@gitam.in*
[2]*Professor, Department of Computer Science and Engineering, GITAM University, Visakhapatnam, India, sprasad@gitam.edu*

Liver Disease (LD) is considered as one of the primary death causes around the world affecting a vast amount of people. A group of factors trouble the liver leads to make dysfunction. The detection of this condition becomes tiresome and costly. There are numerous disorders related to the human liver some of them are complex to recognize by employing the data transmitted among the doctor and patient. Inspired by the better knowledge of Artificial Intelligence (AI) in machines, this work concentrated to discover the strategy that can forecast the existence of LD in specific subjects with improved accuracy on the basis of distinct input attributes. Accurate and fast LD prediction permits timely and efficient treatments. Due to the significance of LD and the increase in the amount of people who are troubled by this disease; the work concentrated the LD via deep learning method. Hence, this work proposes an automated model of LD prediction using the adaptive technique. Initially, the benchmark datasets are considered for gathering the required set of images used for subsequent processes. Further, the gathered input images are subjected to the segmentation process, which is accomplished by Optimized Fuzzy C-Means (OFCM). In this OFCM, the parameters are optimally chosen by using the Amplified Hippopotamus Optimization (AHO) algorithm. Finally, the segmented image is fed into the model of Attention Guided Hybrid Network (AGHNet), in which the Graph Convolutional Neural Network (GCNN) is integrated with the Recurrent Neural Network (RNN) for predicting the LD. Further, the proposed work validates with multiple metrics to deliver the desired outcome. Compared with traditional approaches, the recommended prediction model outperforms with the superior

results of early time disease diagnostic approach.
Keywords: Liver Disease Prediction; Semantic Segmentation; Optimized Fuzzy C-Means; Amplified Hippopotamus Optimization; Attention Guided Hybrid Network; Graph Convolutional Neural Network; Recurrent Neural Network.

1. Introduction

The liver is the primary organ in the human body that conducts the performances such as the source of significant proteins, chemical detoxification, and bile production [9]. Nowadays, an important enhancement of numerous LDs has been monitored around the world. In India, due to this disorder, the rate of mortality is 2.4% enhanced from the overall population [10]. There are numerous LDs among that cirrhosis is detected when the liver cells are replaced and injured by the scar tissues. One of the significant conventional ways to recognize LD is to evaluate if the tissue in the liver is malignant by the experienced clinician [11]. But, the experiments displayed that the accuracy decision of nearly 72% can be taken by the normal LD's visual interpretation. Since numerous healthcare centers, diagnosis centers, and hospitals are equipped with advanced computer-aided machines for diagnosis and testing, the timely identification of LD is possible for rapid cure [12]. Some of the causes of LD are genetic anomalies, drug exposure, high alcohol intake, liver fibrosis, fatty liver, and hepatitis infection [13]. The transplantation of the liver is a better treatment plan if the liver has been entirely damaged and there is no possible way to rectify it. The early recognition of LD can support a speedy recovery and therapy [14]. The LD stages are "healthy, fibrosis, cirrhosis, and the final phase is tumor". Recognizing the LD in its timely phases can be complex, even after there is an important injury to the tissue in the liver [15]. This can result in failure to offer correct drugs and treatment. Timely identification of the disorder is important to eliminate this and secure the lives of the patient.

Presently, the liver biopsy stays the best standard for the detection and classification of the disease phase; however, the biopsy is intrusive and hence restricted [16]. Though, non-intrusive examinations for recognizing the LDs are available including “spectroscopy, Magnetic Resonance Imaging (MRI), ultrasound, and Computed Tomography (CT)”, these examinations are primarily applicable to the identification of modern severity [17]. Hepatic elastography, considered for its high accuracy is now a better option for the early examination of LD patients. Liver Stiffness Measurements (LSM) employed as a marker for the severity of the fibrosis, have been ensured to efficiently exclude modern fibrosis with a better value of negative predictive [18]. But, while the LSM is utilized to grade the fibrosis of the liver, its part in forecasting the progression threat between LD patients without the early indications of fibrosis stays limited [19]. Thus, there is an important requirement for better fidelity timely identification, and the prediction of risk for the LD. In numerous automatic manual detection components, the classification mechanisms are common [20]. Because of the truth that the LDs do not clear unit the body organ is partially injured, it is complex to recognize timely. The enzyme's existence in the blood is employed to recognize the LD [21]. In addition, the mobile systems are highly being employed to monitor the human health. In this case, it is also significant to employ the automatic classification mechanisms [22]. The online and mobile technologies can recognize the LD automatically that minimizes the waiting time of the patients with liver experts including endocrinologists.

The machine learning mechanisms can improve the decision support of the clinical centers by providing less time utilization yet still precise and efficient prediction of liver tumors and fibrosis [23]. Employing statistical evaluation and AI to forecast and detect the rich patterns in numerous data sources, machine learning mechanisms are employed to forecast hepatic disorders. Deep learning is a very improved version of machine learning techniques [24]. Nowadays, deep learning outperforms conventional machine learning strategies with an effective margin in image identification. As a significant model of deep learning, the Convolutional Neural Network (CNN) has illustrated power for the automated explanation of healthcare imagery, employing huge data sources of annotated images for the training process. Presently, the efficacy of the CNNs in categorizing the liver fibrosis phases is highly detected, significantly in the correct detection of cirrhosis of the liver [25]. The experiments have employed CNNs to prevent manual intervention without improved fibrosis, though the model's functionality demands further improvement. However, there is an important requirement for further development in locating the variations in the threat of fibrotic enhancement over time.

The recommended LD prediction approach’s contributions are provided below.

To design an efficient LD prediction approach by utilizing the fuzzy and deep learning concepts that prevent the traditional LD prediction models and improve the efficiency. Moreover, this approach supports the medical experts to perform treatments timely without any false alarms for securing the patient's life.

To suggest an OFCM model by incorporating the FCM with AHO that performs the image segmentation process with higher accuracy. Additionally, this network increases the image quality for performing the LD prediction task.

To develop an AHO model by inheriting the specific features of classical HO and an intelligent strategy that supports the segmentation process for tuning the FCM parameters and also provides the optimal solutions.

To build the AGHNet technique by combining the attention-guided model, GCNN, and RNN that predicts the LD quickly and accurately. This network utilizes necessary image features and minimizes the parameter utilization that increases the uniqueness of the model.

The presented LD prediction system contains the following divisions. The traditional LD prediction models are explained in Division II. The liver disease prediction using adaptive segmentation and classification model with image details are provided in Division III. The optimized clustering mechanism for abnormal segmentation to predict the liver disorder is illustrated in Division IV. The AGHNet for LD prediction is demonstrated in Division V. The experimental validation is given in Division VI and the summary of the recommended LD prediction approach is in Division VII.

2. Existing Works

2.1 Related Works

In 2024, Dai et al. [1] have developed an improved deep learning framework that combined ultrasound elastography images with medical data, improving the prediction process of fibrotic growth in patients. In this analysis, the patients were split into testing and training data sources and finally categorized on the basis of the disease progression. The experiments showed the improved values of the recognition process.

In 2020, Yao et al. [2] have recommended a Densely linked Deep Neural Network (DNN) for screening the LD. The model was experimented on the data source with a huge sample and the functionality of the designed model provided highly better outcomes than the classical systems.

In 2021, Afrin et al. [3] have suggested an LD diagnosis process employing the supervised machine learning approaches. Moreover, the authors utilized the feature selection strategy on the data source to recommend relatively correlated factors of LD. The evaluation was conducted for the prediction process. The experiments displayed a significant improvement in the recommended model.

In 2021, Wong et al. [4] have discussed the concepts of AI on liver images, electronic medical records, and liver biopsies. General AI mechanisms for the single time stamp, sequential data, images, and histology. The research experiments displayed enhanced performance on the LD diagnosis.

In 2022, Dalal et al. [5] have offered an effective model for the timely identification of LD employing the hybrid machine learning model with parameter optimization. The outcomes explained that the chi-squared automated identification of interaction and classification models provided higher accuracy rates that were better than the existing techniques. The designed model supported the physicians in preventing LD.

In 2020, Liu et al. [6] have encouraged the gut metagenomics power clinical validity to complement the existing risk attributes for LD prediction. The experts examined the gut microbiome's clinical validity to enhance the future LD's prediction. The experts illustrated that the traditional risk factor techniques and the gut microbiome provided the same prediction functionalities, yet significantly, the microbiome-augmented traditional risk attribute techniques notably enhanced the prediction. The outcomes displayed that the integration of existing risk attributes with the gut microbiome might have the power in timely risk stratification of the LD.

In 2020, Hashem et al. [7] have implemented prediction techniques using machine learning for Chronic Hepatitis C (CHC). The machine learning techniques including regression tree employed to construct the HCC categorization techniques for forecasting the presence of HCC. The recommended technique offered sufficient diagnosis solutions.

In 2023, Md et al. [8] have designed an improved pre-processing and ensemble learning to forecast the LD. The recommended technique employed some pre-processing strategies for improving the accuracy. Then the data was trained on the various machine learning approaches. The outcomes contrasted with other existing frameworks.

2.2 Research Gaps and Challenges

The LD refers to any pathology that destroys or harms the liver or eliminates it from normal processing. The global society has monitored an enhancement in the rate of mortality to LD.

This can be characterized by numerous attributes, among that are human habits, late identification, poor healthcare, and awareness issues. To prevent the developing problems from LD, timely recognition is a crucial part to minimize the threats and enhancing the treatment solutions. In the past few days, multiple automatic mechanisms have been constructed to forecast the LD in early times. However, the techniques have some major difficulties, and that are listed below. Table 1 depicts the merits and drawbacks of existing LD prediction systems.

o To predict the LD at the correct time is significant. The manual prediction models are susceptible to error and always demand experienced specialists. Therefore, an efficient automated LD prediction model is crucial.

o The majority of the existing LD prediction frameworks employ machine learning models that are computationally intensive and lack proper interpretation. Therefore, implementing a deep learning-aided LD prediction system is significant.

o Some of the existing LD prediction frameworks didn't consider the segmentation process before predicting the LD. This minimized the quality of the images and consumed more time. Hence, a powerful segmentation strategy is necessary to improve the image quality and minimize the computation time.

o Although some conventional models consider the abnormality segmentation process, these works hardly perform the parameter tuning of these segmentation networks. This increased the dimensionality issues. Therefore, a new optimization mechanism is important for tuning the parameters of the segmentation process.

o Some of the classical LD prediction models employ single deep learning models for predicting the LD. However, these models can't give satisfactory outcomes and also encounter network overhead issues. To overcome these difficulties a hybrid deep network is significant for predicting the LD.

Therefore, a new LD prediction approach is designed in this work to overcome the existing technique's limitations.

Table 1. Features and challenges of traditional LD prediction model

Author [citation]	Methodology	Features	Challenges
Dai et al. [1]	ResNet-50	• It learns the effective feature representations. • It is simple to optimize and has low training time.	• It is computational resource is high and faces overfitting issues.
Yao et al. [2]	DenseDNN	• It increases the generalization and provides high accuracy. • It efficiently handles the large data sources.	• It is susceptible to vanishing gradient issues and utilizes large parameters.
Afrin et al. [3]	SVM	• It is very flexible and robust to noise. • It handles the overfitting issues.	• It can't handle complex and large datasets.
Wong et al. [4]	XGBoost	• It handles imbalanced data sources and gives higher accuracy.	• It consumes more memory power while handling large datasets.

		• It offers interpretable outcomes and handles the missing values in the datasets efficiently.	
Dalal et al. [5]	XGBoost	• It is very fast and simple to develop. • It automatically selects the significant features.	• It is not applicable to small-sized data sources.
Liu et al. [6]	XGBoost	• Its hyperparameter tuning is simple and minimizes overfitting. • It can process distinct kinds of inputs accurately.	• It is hard to interpret and prone to outliers.
Hashem et al. [7]	Regression tree	• It is simple to understand and visualize. • It is a fast and effective mechanism.	• It cannot handle the missing values properly.
Md et al. [8]	Random Forest	• It accurately handles high dimensional data. • It is robust to noisy data.	• It is not applicable in real time.

3. Liver Disease Prediction Using Adaptive Segmentation and Classification Model with Image Details

3.1 Illustration of Novel Liver Disease Prediction

LD is caused by the swelling nature of the liver created by an inherited disorder, bacteria, or toxic substances that make the liver not work correctly as it is significant for digestion and eliminating the bacteria. When the LD is detected at a timely phase, among the infection and fibrosis yet prior to cirrhosis, liver injury is prevented. Liver-based disorders cause 70% mortality rates. There is a requirement to discover better ways to recognize and detect the LD with better accuracy. Especially, the experiments on liver function require to be affordable and available to sick persons. In order to rectify the invasive and expensive experiments, machine learning techniques are introduced in the medical sector. The utilization of these techniques permits timely identification and highly avoids numerous LD cases from developing to the extent of requiring complex and biopsy treatment. The algorithms of machine learning are new strategies to manage numerous hidden issues in the data sources. This strategy supports the healthcare sector and experts to discover better solutions for various clinical applications. In the medical sector, discovering the proper target and the features are highly complex for the classification issues. The logistic regression is a highly employed model, yet its functionality is highly lower than the some models of machine learning and deep learning. Employing machine learning approaches to forecast the disease is made possible by improving access to the hidden parameters in the healthcare data source. However, existing machine learning algorithms still need enhancements for forecasting the LD with maximum accuracy rates. Since deep learning offers more satisfactory solutions in the medical sector than conventional machine learning algorithms, there is a requirement for developing the deep learning-based LD prediction process. The overall process of the suggested LD prediction system is pictorially given in Fig.1.

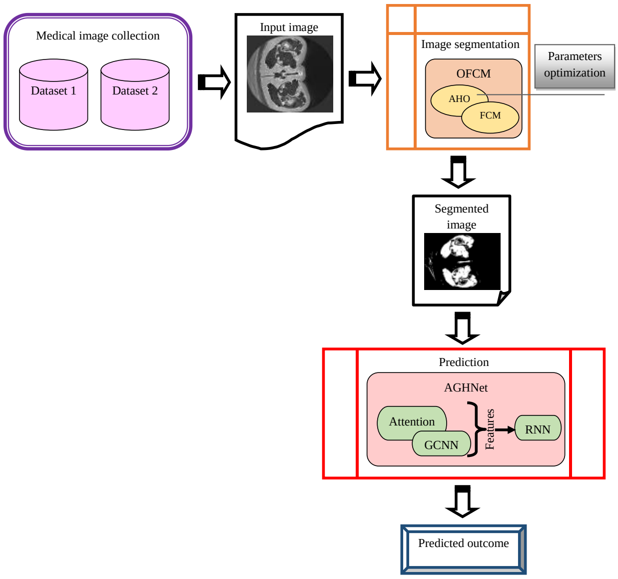

Fig. 1. Pictorial illustration of designed LD prediction model

An automated LD prediction system is introduced in this work by presenting the deep learning concept. At first, from the distinct data sources, the necessary images are taken and employed for the subsequent tasks. After that, the obtained images are forwarded to the segmentation task, where the OFCM technique is supported for segmenting the irregularities. Additionally, this phase includes the newly recommended AHO model optimizing the FCM attributes, thus it is maximizing the accuracy. Subsequently, the segmented image is then taken to the disease prediction process, where the AGHNet technique is utilized. In this process, the GCNN, attention guided model, and RNN techniques are integrated. The attention-based GCNN is utilized for grasping the significant features and then the features are fed into the RNN technique for producing the accurate and timely prediction. Finally, the validation for the designed LD system is conducted to showcase the enhanced functionality of the system.

3.2 Image Collection Details

The following data sources are employed for analyzing the developed LD prediction model.
Dataset 1 ("Liver Tumor Segmentation"): From the Kaggle, using the link "https://www.kaggle.com/datasets/andrewmvd/liver-tumor-segmentation: access date: 2024-07-12", the medical images are gathered. This data source has 130 CT scans. There are 182 files present in this source and this is the fifth version of this source.
Dataset 2 ("Medical Segmentation Decathlon"): The dataset is considered for the developed model via "http://medicaldecathlon.com/: access date:2024-07-12". This dataset also has CT images, where 70 images are utilized for testing and 131 images are utilized for training. The images are present in 3D volumes.
From this dataset, the fetched medical images are represented as L_m, $here\ m = 1,2,...,M$. The gathered medical image's total count is specified as M. The sample images taken for the developed LD prediction are given in Fig. 2.

Images	1	2	3	4	5
“Dataset 1”					
“Normal”	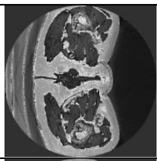	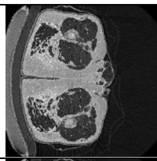	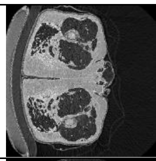	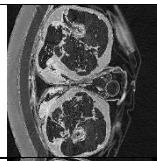	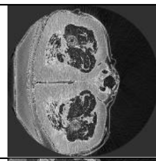
“Abnormal”	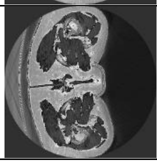	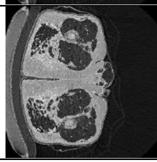	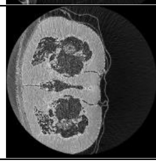	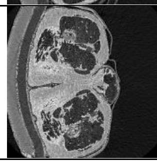	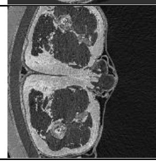
“Dataset 2”					
“Normal”	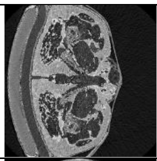	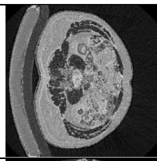	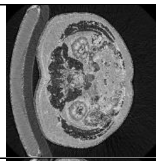	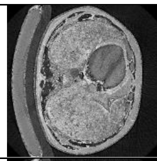	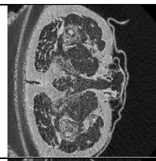
“Abnormal”	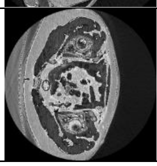	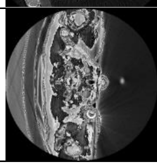	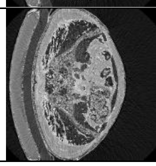	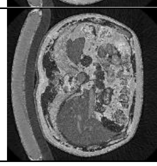	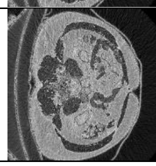

Fig. 2. Sample images of the developed LD prediction model

3.3 New Heuristic Algorithm: AHO

To perform the segmentation process effectively, the AHO is implemented in this work.
Purpose: The AHO is the modified algorithm of HO. The AHO helps to optimize the attributes in the FCM such as fuzziness parameter, number of iterations, and epsilon. Moreover, the AHO helps to maximize the accuracy in the segmentation process.
Novelty: The designed AHO utilizes the conventional HO for discovering the optimal outcomes with a new concept. The HO employs the hippopotamus’s escaping and defense strategies. The HO gives highly efficient solutions and also it is suitable for complex optimization problems. However, the existing HO includes more random variables that consume more time to complete the iteration process. This may affect the convergence rates. Hence, a new random variable is designed to prevent this issue. Thus, the HO is improved and named AHO. The new random factor in the AHO is on the basis of iteration counts. Therefore, the iteration process is improved with this random factor thus improving the overall efficiency. The newly modified random attribute y_{10} is given in Eq. (1).

$$y_{10} = -i * \left(\frac{(-1)}{I} \right) \tag{1}$$

In this, the present iteration is specified as i, and the highest iteration is provided as I. By employing this enhanced arbitrary variable, the AHO is designed and thus provides very effective solutions. The HO model’s functionalities are presented as follows.

By concentrating on the hippopotamuses, and relevant features, the HO is designed. There are three distinct hippopotamus behaviors considered in the existing HO such as:

- Exploration: Hippopotamus's position upgrading on the basis of river or pond.
- Exploration: Defence strategy of hippopotamus over hunter.
- Exploitation: Escaping strategy of hippopotamus from the hunter.

These phases are explained below.

Initialization: In this process, by utilizing Eq. (2), the decision attribute is generated.

$$r_j : r_{jk} = m_k + y.(v_k - m_k),\ j = 1,2,...,A;\ k = 1,2,..,d \qquad (2)$$

Here, the k^{th} candidate outcome's region is taken as r_j , and the random factor is considered as y . The size of the population for the hippopotamus is A and the "lower and upper" regions are m_k *and* v_k . The count of the decision factor is given as d . The population matrix is provided in Eq. (3).

$$R = \begin{bmatrix} R_1 \\ \vdots \\ R_j \\ \vdots \\ R_A \end{bmatrix}_{A\times d} = \begin{bmatrix} r_{1,1} & \cdots & r_{1,k} & \cdots & r_{1,d} \\ \vdots & \ddots & \vdots & \therefore & \vdots \\ r_{j,1} & \cdots & r_{j,k} & \cdots & r_{j,d} \\ \vdots & \therefore & \vdots & \ddots & \vdots \\ r_{A,1} & \cdots & r_{A,k} & \cdots & r_{A,d} \end{bmatrix}_{A\times d} \qquad (3)$$

Exploration-Hippopotamus's position updating: This stage's position updating is performed Eq. (4).

$$R_j^{Dhippo}; r_{j,k}^{Dhippo} = r_{j,k} + b_{1.}\left(Xhippo - J_1 r_{j,k}\right)$$
$$for\ \ j = 1,2,...,\left\lceil \frac{A}{2} \right\rceil\ and\ \ k = 1,2,...,d \qquad (4)$$

In this, the male hippopotamus is taken as R_j^{Dhippo} , and the arbitrary factor is viewed as $\vec{y}_{1,...,4}$ among the range of 0 and 1. The region of the dominant hippopotamus is considered as $Xhippo$. The arbitrary integer is given as J_1 *and* J_2 . The factors J_1 *and* J_2 explain the integer between 1 and 2. Some of the randomly selected hippopotamus's mean value is given as dT_i . The factor b_1 is also arbitrary. Then, the random values that can be one or zero are taken as Q_1 *and* Q_2 .

$$f = \begin{cases} J_2 \times \vec{y}_1 + (\sim Q_1) \\ 2 \times \vec{y}_2 - 1 \\ \vec{y}_3 \\ J_5 \times \vec{y}_5 + (\sim Q_2) \\ \vec{y}_5 \end{cases} \qquad (5)$$

$$I = \exp\left(-\frac{c}{I}\right) \qquad (6)$$

$$R_j^{ghippo} : r_{j,k}^{ghippo} = \begin{cases} r_{j,k}\, f_1.\left(Xhippo - J_2.dT_j\right) & J > 0.6 \\ \Xi & else \end{cases} \qquad (7)$$

$$\Xi = \begin{cases} r_{j,k} + f_2.(dT_j - Xhippo), & y_6 > 0.5 \\ m_k + y_7.(v_k - m_k), & else \end{cases}$$
$$for \ \ j = 1,2,\ldots,\left[\frac{A}{2}\right], k = 1,2,\ldots,d \qquad (8)$$

In this, the region of the naïve hippopotamus is determined by employing Eq. (7) and Eq. (8). The female hippopotamus has separated from its mother if the value of the factor I is greater than 0.6. The female hippopotamus has separated from its mother yet still stays in the herd if the value of the factor I is greater than 0.5. The region upgrading of female or naive and male hippopotamus is performed by Eq. (9) and Eq. (10). Here, the objective function value is W_j.

$$W_j = \begin{cases} R_j^{Dhippo} R_j^{Dhippo} & < W_j \\ R_j & else \end{cases} \qquad (9)$$

$$W_j = \begin{cases} R_j^{khippo} R_j^{khippo} & < W_j \\ R_j & else \end{cases} \qquad (10)$$

Exploration-Defense strategy of hippopotamus: One of the primary reasons for the herd living of hippopotamus is safety and security. The hunter's position in the search region is determined by Eq. (11).

$$predator : predator_k = m_k + \vec{y}_8.(v_k - m_k), l = 1,2,..,d \qquad (11)$$

In this, the variable $\vec{y}_8$ is an arbitrary factor.

$$\vec{X} = \left| predator_k - r_{j,k} \right| \qquad (12)$$

Eq. (13) estimates the distance of the i^{th} hippopotamus to the hunter.

$$R_j^{hippoY} : r_{j,k}^{hippoY} =$$
$$\begin{cases} Y\vec{M} \oplus predator_k + \left(\frac{\vec{s}}{(\sigma x \times \cos(2\pi k))}\right).\left(\frac{1}{\vec{X}}\right), & W_{predator_j} < W_j \\ Y\vec{M} \oplus predator_k + \left(\frac{\vec{s}}{(\sigma x \times \cos(2\pi k))}\right).\left(\frac{1}{2 \times \vec{X} + y_9}\right), & W_{predator_j} \geq W_j \end{cases} \qquad (13)$$
$$for \ \ j = \left[\frac{A}{2}\right] + 1, \left[\frac{A}{2}\right] + 2, \ldots, A \ \ and \ \ k = 1,2,\ldots,d$$

In this, the hippopotamus's region is considered as R_j^{hippoY}. The factor is indicated as $Y\vec{M}$. The Levy movement's random motion is estimated by Eq. (14).

$$Levy(H) = 0.05 \times \frac{e \times \sigma_e}{|h|^{\frac{1}{h}}} \qquad (14)$$

$$\sigma_e = \left[\frac{\Gamma(1+h)\sin\left(\frac{\pi h}{2}\right)}{\Gamma\left(\frac{1+h}{2}\right) H \, 2^{\frac{(h-1)}{2}}}\right] \qquad (15)$$

The arbitrary factor from two to four is taken as s and the arbitrary factor from two to three is X. The local minima problem is reduced by Eq. (16).

$$W_j = \begin{cases} R_j^{hippoY} R_j^{hippoY} & < W_j \\ R_j W_j^{hippoY} & \geq W_j \end{cases} \tag{16}$$

Exploitation-Escaping strategy of hippopotamus: This stage is estimated from Eq. (17) to Eq. (20). Here, the highest and present iteration is provided as $I \;\; and \;\; i$.

$$m_k^{local} = \frac{m_k}{i}, v_k^{local} = \frac{v_k}{i}, i = 1,2,\ldots,I \tag{17}$$

$$R_j^{hippo\delta} : r_{j,k}^{hippo\delta} = r_{j,k} + y_{10} \cdot \left(m_k^{local} + j_1 \cdot \left(v_k^{local} - m_k^{local} \right) \right)$$
$$for \;\; j = 1,2,\ldots,A, \; k = 1,2,..,d \tag{18}$$

$$j = \begin{cases} 2 \times \vec{y}_{11} - 1 \\ y_{12} \\ y_{13} \end{cases} \tag{19}$$

$$W_j = \begin{cases} R_j^{hippo\delta} R_j^{hippo\delta} & < W_j \\ R_j W_j^{hippo\delta} & \geq W_j \end{cases} \tag{20}$$

In this, the hippopotamus's region, which is near to the safe place, is considered as $R_j^{hippo\delta}$. Among the three criteria, the chosen random factor is given as j_1. The upgraded random variable is y_{10}. The factors $\vec{y}_{11} \;\; and \;\; \vec{y}_{13}$ are random integers. Algorithm 1 shows the AHO's pseudo-code.

Algorithm 1: Developed AHO

Define the problem of optimization
Consider the maximum iteration I and hippopotamus count A
Generate population of hippopotamus and determine fitness function
For $i = 1 \;\; to \;\; I$
    For $j = 1 \; to \;\; A$
        New random factor estimation by Eq. (1)
        Exploration-position updating
        New region estimation for hippopotamus by Eq.(4) and Eq. (7)
        Hippopotamus region updating by Eq. (9) and Eq. (10)
        Exploration-Defense strategy
        Generate random region for hunters by Eq. (11)
        New region estimation for hippopotamus by Eq.(13)
        Hippopotamus region updating by Eq. (16)
        Exploitation: Escaping strategy
        New region estimation for hippopotamus by Eq.(18)
        Hippopotamus region updating by Eq. (20)
    End for
    Save the best outcome
End for
Return the optimal solution

4. Optimized Clustering Mechanism for Abnormal Segmentation to predict the Liver Disorder

4.1 Fuzzy C Means Clustering

The FCM [27] technique is defined as a group C in l clusters. It has candidates M from $C = c_1, c_2, c_3, .c_4$. It is reported that the data's c_1 uncertain phase was divided into some clusters by numerous membership degrees v_{mn}. The cluster data's membership is estimated by paralleling its dissimilarity or distance from the centroid of the cluster w_n to e_{mn}. The validations of distance are carried out by the Euclidean formula by Eq. (21).

$$FCM = \sum_{n=1}^{l} \sum_{m}^{M} v_{mn}^{q} e_{mn}^{2} \tag{21}$$

Here, $q \in (1, \infty)$ *and* $\sum_{n=1}^{l} e_{mn} = 1$.

The fuzzifier attribute's q job is to mechanize the degree of membership handle over the fitness function. The degree value and the membership centroid were determined in Eq. (22) and Eq. (23) correspondingly.

$$v_{mn} = \frac{1}{\sum_{r=1}^{l} \left(\frac{e_{mn}^{2}}{e_{mr}^{2}} \right)} \tag{22}$$

$$v_{n0} = \frac{\sum_{m=1}^{O} v_{mn}^{q} y_m}{\sum_{m=1}^{O} v_{mn}^{q}} \tag{23}$$

4.2 Developed OFCM for Segmentation

The OFCM is presented for performing the segmentation process. The FCM has a high identification rate and a very minimal false location rate. Besides, the model is very effective for the medical image segmentation process. However, in critical times, the FCM can't properly handle the uncertainty in the cluster assignments. Therefore, tuning the fuzziness is necessary in the FCM technique. Additionally, the FCM and the number of iterations also need to be tuned properly for achieving highly accurate and correct segmented images. To perform this tuning process, the AHO is recommended since it can capture the optimal solutions in less amount of time with better convergence. Thus, the OFCM network is constructed for performing medical image segmentation. In this network, the gathered medical images L_m are taken as input. The objective function is given in Eq. (24).

$$ob = \underset{\{fz^{fcm}, ep^{fcm}, It^{fcm}\}}{\arg\min} \left[\frac{1}{Ac} \right] \tag{24}$$

Here, the fuzziness attribute in the FCM is given as fz^{fcm} varies from [2-20]. The epsilon in the FCM is given as ep^{fcm} varies from [1-20]. The number of iterations in the FCM is given as It^{fcm} varies from [10-100]. The factor Ac is the accuracy that recognizes the relationship among the original and segmented images. It is expressed in Eq. (25).

$$Ac = \frac{vv + hh}{vv + gg + ss + kk} \tag{25}$$

In this, the "true negative and true positive values" are represented as gg *and* kk. The "false negative and false positive values" are represented as vv *and* ss. Finally, the segmented images are achieved by the OFCM method and the segmented image is pointed as L_m^{seg}. The OFCM-based segmentation process is shown in Fig.3.

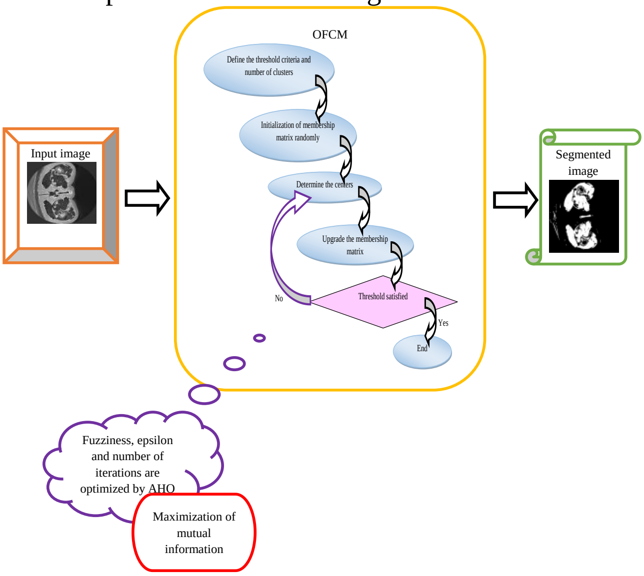

Fig. 3. Illustration of OFCM-based segmentation process

5. Attention Guided Hybrid Network with GCNN and RNN for Liver Disease Prediction

5.1 Graph Convolution Neural Network

The GCNN [28] technique is implemented for executing the graph-structured data. To generate the GCNN, an adjacency matrix for the graph is developed. For instance, in the non-oriented model $B_{jk} = 1$, if and only if there is a link among the nodes j *and* k and $B_{jk} = 0$ also if only if j *and* k are disjoint. Further, the node matrix is generated and next the matrix is displayed in Eq. (26).

$$I' = \sigma\left(\hat{E}^{-1}\hat{B}IX\right) \tag{26}$$

Here, the none-by-node distributed sequential transformation that is learned is given as X, and the non-linear function is taken as σ such as Rectified Linear Unit (ReLU). Then $\hat{B} = B + 1$, and degree matrix is considered as $\hat{E}$. It is considered as the mean-pooling update condition. Eq. (27) gives the symmetric normalization.

$$I' = \sigma\left(\hat{E}^{-1/2}\hat{B}^{-1/2}IX\right) \tag{27}$$

The next task is to assign the update condition for the GCN. This GCN is normally utilized. In the improved framework, the nodes send any message along the nodes $\vec{f}_{jk}$ further the node fetches the overall obtained measures employing the permutation invariant function. Consider $\overline{n}_{jk}$ be the message sent from the node to node estimated in Eq. (28) employing the message function g_f.

$$\vec{n}_{jk} = g_f\left(\vec{h}_j, \vec{h}_k, \vec{f}_{jk}\right) \quad (28)$$

By employing the readout function in Eq. (29), the overall massages entering a node are gathered.

$$g_w = \vec{i}_j^{'} = g_w\left(\vec{i}_w, \Sigma_{k \in M_j} \vec{o}_{kj}\right) \quad (29)$$

Here, the node j neighbor's collection is given as M_j. The variables g_f *and* g_w are small multilayer perceptrons. Eq. (30) gives the normal version.

$$\vec{i}_j^{'} = \sigma\left(\Sigma_{k \in M_j} \sigma_{jk} X \vec{i}_k\right) \quad (30)$$

Here, the factor σ_{jk} is either a defined coefficient that has several drawbacks or

$$\sigma_{jk} = \frac{\exp\left(b_{jk}\right)}{\Sigma_{k \in M_j} \exp\left(b_{jk}\right)} \quad (31)$$

Here,

$$b_{jk} = b\left(\vec{i}_w, \vec{i}_k, \vec{f}_{mk}\right) \quad (32)$$

The factor b is learned via a distributed self-attention strategy. The architecture of the GCNN is provided in Fig.4.

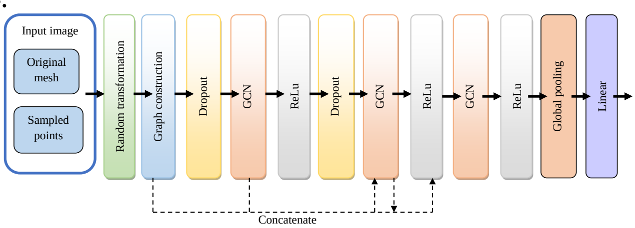

Fig. 4. Architecture of GCNN for LD prediction

5.2 Recurrent Neural Network

The RNN [29] is a powerful neural network that manages medical images efficiently. In contrast to the MLP, the RNN technique is considered as very simple and also learns the significant parameters, which are named hidden states. According to the hidden states, the RNN precisely manages the sequential information. In the training process, the hidden states are upgraded on the basis of both current and historical information of the sequential data. The recurrent layer's hidden state f_d and the outcome h_d, where $d \in \{1, \ldots, D\}$ specifies the frame index are determined by Eq. (33) and Eq. (34).

$$f_d = \tanh\left(S_{ff} f_{d-1} + S_{tf} + k_f\right) \quad (33)$$

$$h_d = S_{fh} f_d + k_h \quad (34)$$

Here, the biases and weights are considered as k *and* S accordingly among elements. The RNN's functional diagram is depicted in Fig.5.

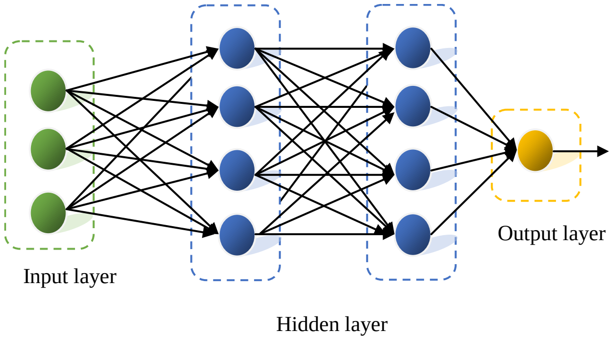

Fig. 5. Functional diagram of RNN for LD prediction

5.3 Suggested AGHNet for Prediction

The AGHNet is developed for predicting the LD. This network includes the attention mechanism, GCNN, and RNN models. The GCNN technique is highly capable to handle the graph-structured data and efficiently learning the features. Moreover, it increases the generalization. Though this network is effective, this model demands additional methods to provide competitive performance. In order to improve the feature learning task's performance in the GCNN model, the attention method is included. The attention technique [30] is normally employed to improve the accuracy of the process by concentrating the related features. It allows the model to concentrate on specific regions of the given images and provides significant features and ignoring the irrelevant ones. In this work, the attention model is applied toward the outcome of the GCNN layers leads to concentrate highly relevant features and also increases the GCNN model's effectiveness. The attention method is shown in Eq. (35).

$$Attention\left(c,h,r\right)=soft\max\left(k\left(ch^{T}\right)\right)r \tag{35}$$

Here, the "key, value, and query" matrices are represented as $h, r,$ *and* c accordingly. Thus, the GCNN is guided by the attention method. The attention-guided GCNN model effectively selects the necessary image features. However, the model can't predict the LD accurately since this network can't properly remember the previous features. Therefore, the RNN technique is combined with this model for providing highly accurate prediction outcomes. This technique can remember past image features and is also effective to handle vast features. Thus, the model becomes AGHNet. In this network, initially, the segmented images L_m^{seg} are processed as input for the attention-guided GCNN model. This network properly recognizes the related features and eliminates the unwanted attributes from the segmented images. Subsequently, the extracted necessary features from the attention-guided GCNN are forwarded to the RNN technique. Here, this network predicts the LD without any errors. Finally, the AGHNet technique produces the LD-predicted outcome accurately. The AGHNet-based LD prediction process is shown in Fig.6.

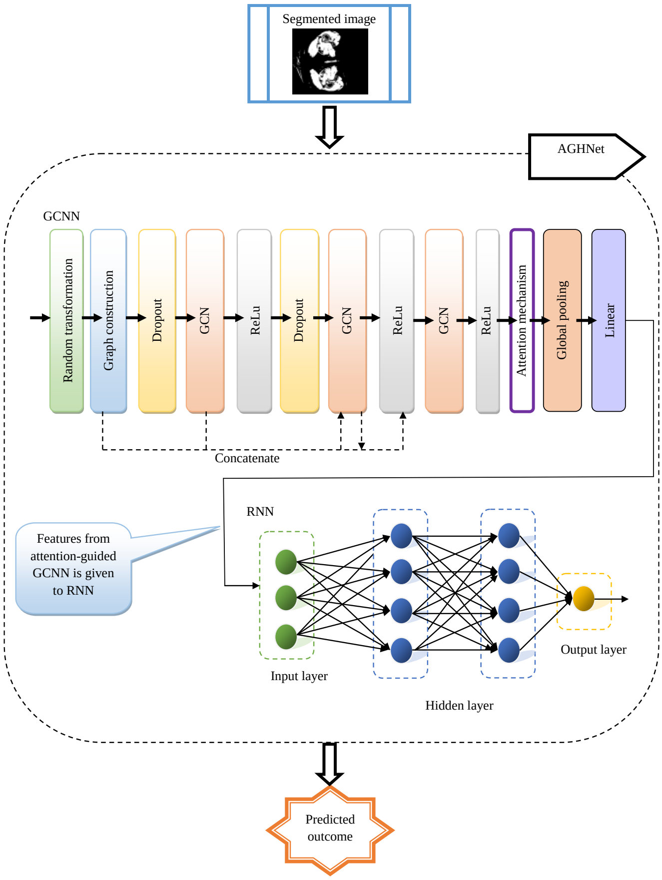

Fig. 6. Illustration of AGHNet-based LD prediction

6. Results and Discussions

6.1 Experimental Setup

The presented LD prediction process was implemented by the Python platform. The AHO utilized 10 populations and a maximum of 50 iterations. Additionally, the length of the chromosome for the AHO was 3. Several optimization models such as “Rat Swarm Optimizer (RSO) [31], Dwarf Mongoose Optimization (DMO) [32], Osprey Optimization Algorithm (OOA) [33], and HO [26]” and some of the traditional segmentation models such as “Active Contour [34], Binary Thresholding [35], K-Means Clustering (KMC) [36], and FCM [27]” were utilized for the experiment. Some conventional classifiers such as “Mobilenet [37], Shufflenet [38], CNN [39], and GCNN [28]” were taken for evaluation.

6.2 Resultant images

The OFCM technique is supported for the segmentation process and the desired solutions are obtained. The resultant images of the designed process are offered in Fig.7.

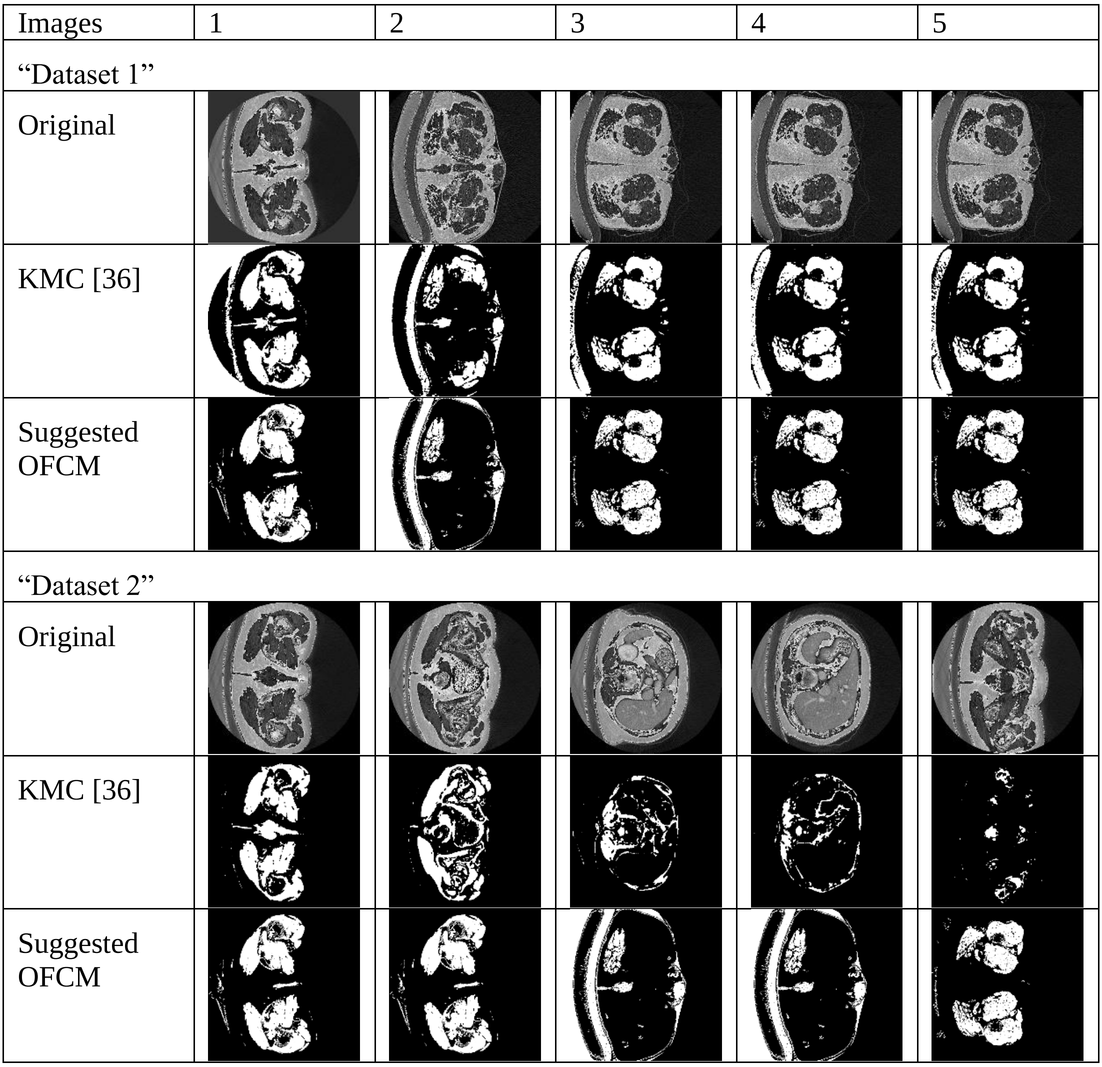

Fig. 7. Resultant images of presented OFCM-based segmentation process over the conventional technique

6.3 Experimental measures

The designed LD prediction system employed the following experimental measures for the evaluation.

Accuracy: It is determined in Eq. (25).

PSNR: It is determined in Eq. (36).

$$PSNR = 10 \log_{10}\left(\frac{\max_L^2}{MSE}\right) \tag{36}$$

MSE: It is determined in Eq. (37).

$$MSE = \frac{1}{B}\sum_{b=1}^{B}\left(L_m - \hat{L}_m\right)^2 \tag{37}$$

Coefficient of similarity: It is determined in Eq. (38).

$$cs\left(L_m, L_m^{seg}\right) = \frac{\left(L_m \cap L_m^{seg}\right)}{\left(L_m \cup L_m^{seg}\right)} \tag{38}$$

Sensitivity: It is determined in Eq. (39).

$$Sen = \frac{vv}{vv + hh} \tag{39}$$

FPR: It is determined in Eq. (40).

$$FPR = \frac{ss}{ss + vv} \tag{40}$$

MK: It is determined in Eq. (41).

$$MK = P + \frac{hh}{(hh + kk)} - 1 \tag{41}$$

TS: It is determined in Eq. (42).

$$TS = \frac{vv}{(vv + ss)} \tag{42}$$

F1 score: It is determined in Eq. (43).

$$F1 - Score = 2 \times \frac{hh \times ss}{hh + ss} \tag{43}$$

Precision: It is determined in Eq. (44).

$$P = \frac{vv}{vv + ss} \tag{44}$$

Spatial overlap: It is employed to validate the spatial overlap among two segmented images.

6.4 ROC experiment of recommended LD prediction

The recommended LD prediction model's ROC estimation is demonstrated in Fig.8 over distinct techniques for two datasets. The efficiency of the LD prediction model is examined with this ROC experiment. The designed LD prediction process is 9.09%, 6.81%, 4.54%, and 2.27% enhanced by Mobilenet, Shufflenet, CNN, and GCNN accordingly for 0.3rd FPR value in Fig.8 (a). This evaluation ensures the designed LD prediction system is highly effective and has lower error values than the conventional techniques.

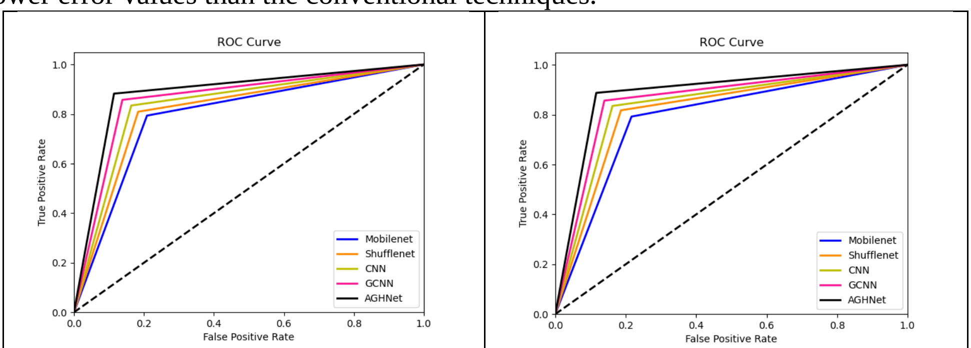

(a) (b)

Fig. 8. ROC experiment of recommended LD prediction over traditional classifiers

concerning " (a) Dataset 1, and (b) Dataset 2"

6.5 Recommended segmentation process's performance examination

The recommended segmentation operation's performance is analyzed by several evaluation metrics for two datasets. Fig. 9 and Fig.10 present the performance investigation for the first dataset over conventional optimization models and segmentation techniques. Fig.11 and Fig.12 provide the performance investigation for the second dataset over traditional optimization models and segmentation techniques. For the 3rd image in Fig.9 (b), the accuracy of the OFCM-aided segmentation task is 7.7%, 10%, 5.5%, and 3.3% increased than the traditional optimization models such as RSO-OFCM, DMO-OFCM, OOA-OFCM, and HO-OFCM respectively. Also, for the 5th image in Fig.12 (a), the spatial overlap of the OFCM-aided segmentation process 13.33%, 2.22%, 11.11%, and 12.22% enhanced than the existing segmentation methods such as Active Contour, Binary Thresholding, KMC, and FCM accordingly. Therefore, it has been explained that the designed segmentation operation outperformed the classical models.

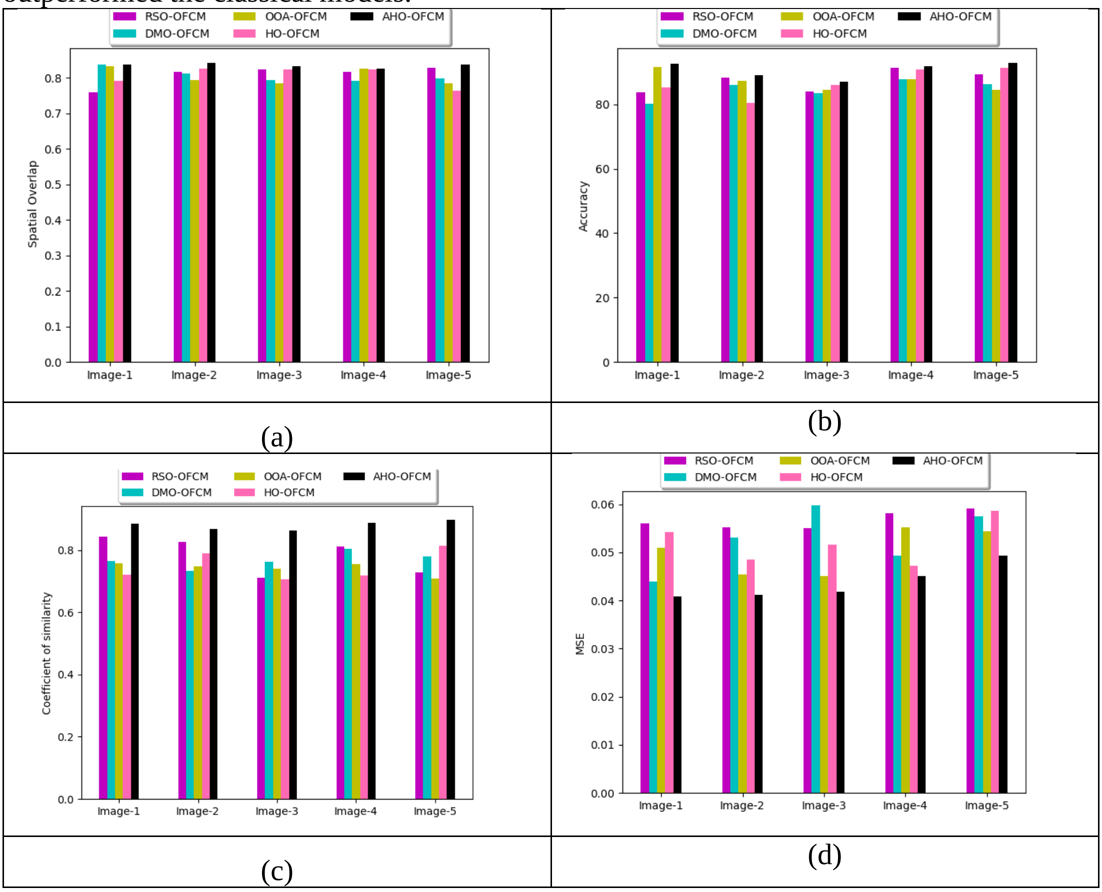

(a) (b)

(c) (d)

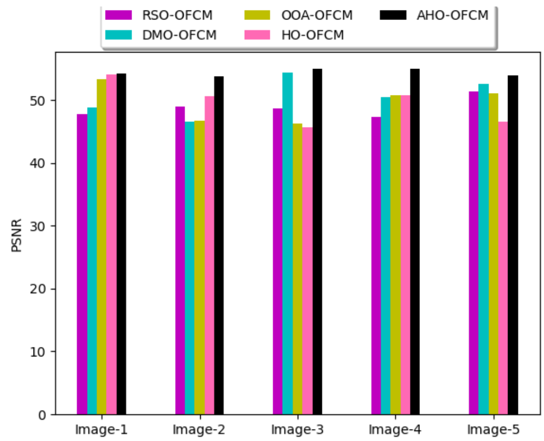

(e)

Fig. 9. Recommended segmentation process's performance examination for the first dataset over traditional optimization models regarding " (a) Spatial overlap, (b) Accuracy, (c) Coefficient of similarity, (d) MSE, and (e) PSNR"

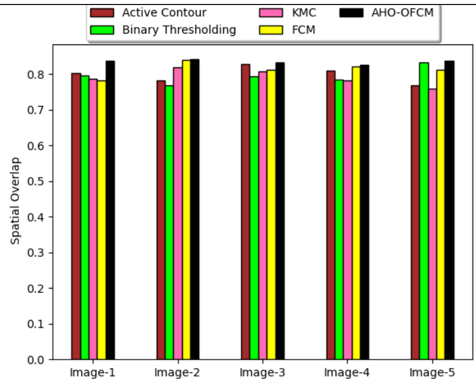

(a)

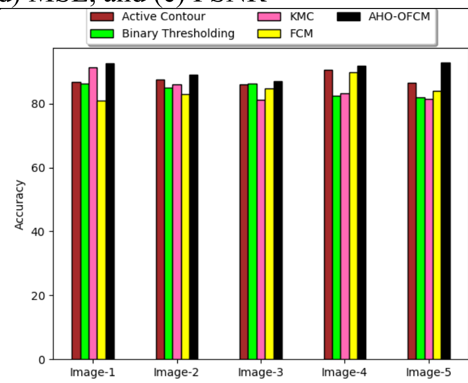

(b)

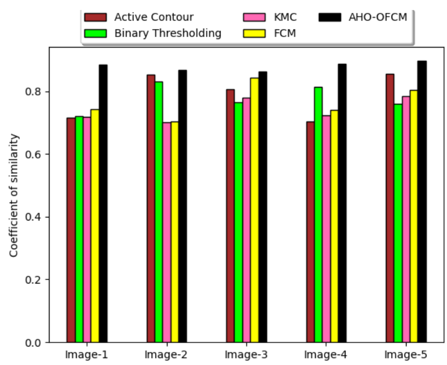

(c)

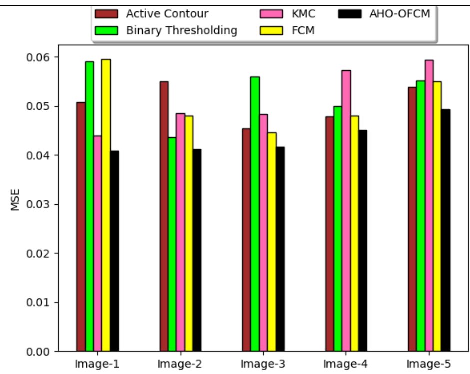

(d)

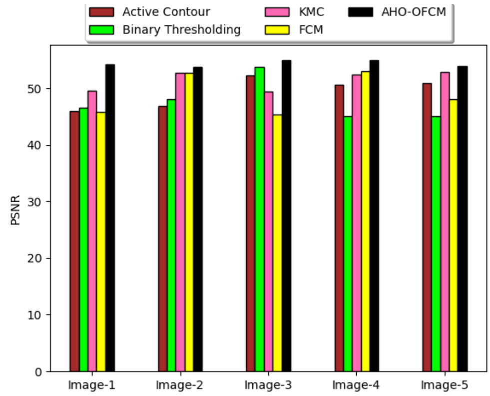

(e)

Fig. 10. Recommended segmentation process's performance examination for the first dataset over traditional segmentation methods regarding "Spatial overlap, (b) Accuracy, (c) Coefficient of similarity, (d) MSE, and (e) PSNR"

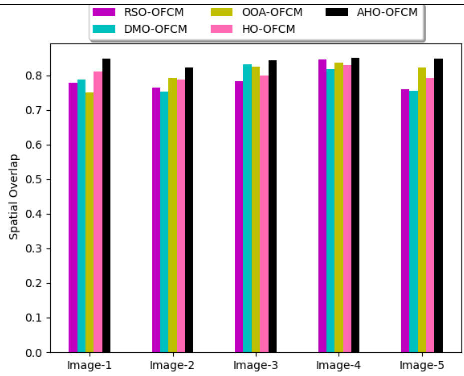

(a)

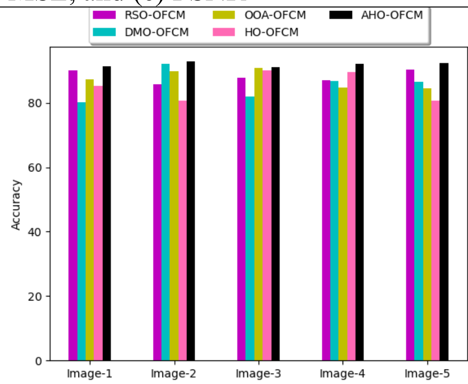

(b)

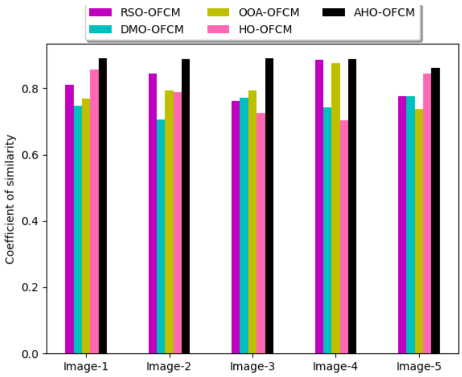

(c)

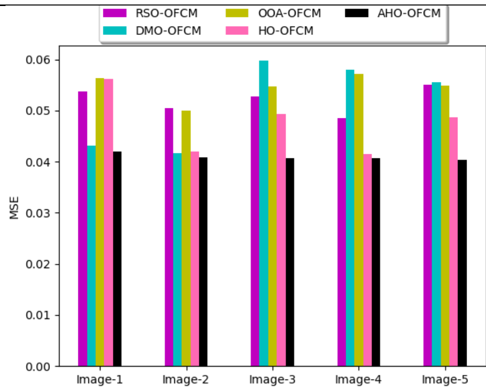

(d)

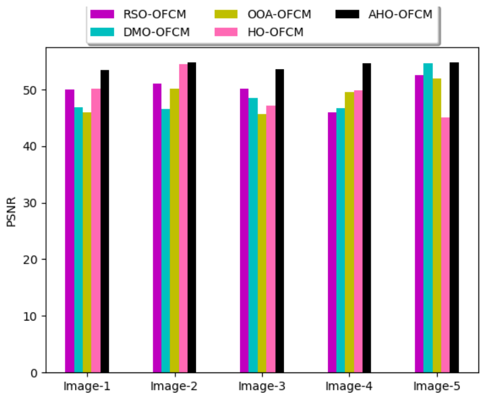

(e)

Fig.11. Recommended segmentation process's performance examination for the second dataset over traditional optimization models regarding "Spatial overlap, (b) Accuracy, (c) Coefficient of similarity, (d) MSE, and (e) PSNR"

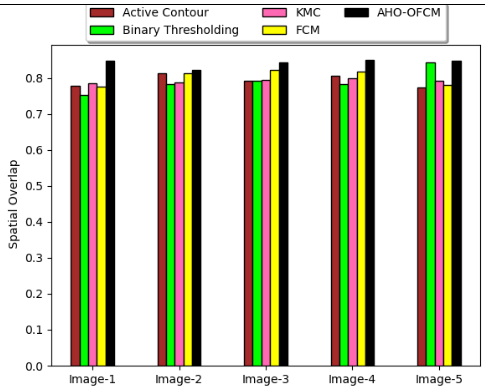

(a)

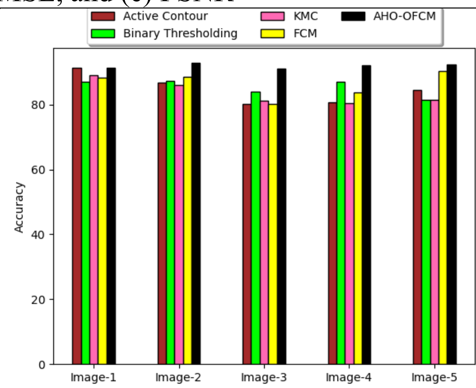

(b)

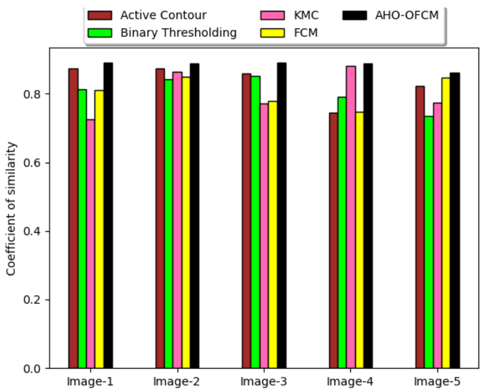

(c)

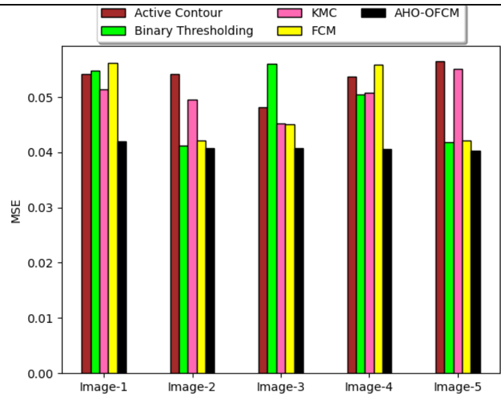

(d)

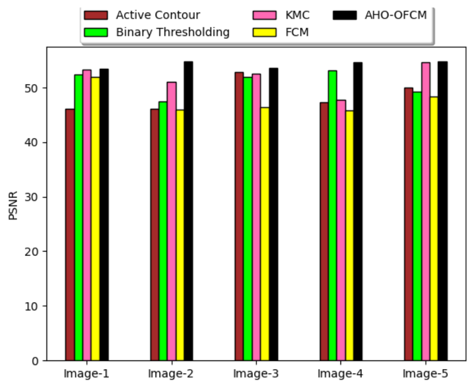

(c)

Fig. 12. Recommended segmentation process's performance examination for the second dataset over traditional segmentation methods regarding "Spatial overlap, (b) Accuracy, (c) Coefficient of similarity, (d) MSE, and (e) PSNR"

6.6 Recommended segmentation process's overall comparative examination

The recommended segmentation operation's overall comparative examination is given in Table 2 and Table 3 for two datasets over traditional algorithms and segmentation strategies. The standard measures are considered in this experiment and showed the enhanced performance of the OFCM strategy. In Table 3, the developed OFCM-aided segmentation process offered 19.10%, 13.48%, 21.34%, and 8.98% higher coefficient similarity values than the conventional segmentation techniques including Active Contour, Binary Thresholding, KMC, and FCM correspondingly. In Table 2, the recommended OFCN-aided segmentation strategy offered 8.6%, 10.1%, 0.16%, and 11.69% improved PSNR values than the traditional optimization algorithms including RSO-OFCM, DMO-OFCM, OOA-OFCM, and HO-OFCM respectively. Therefore, it has been reported that the implemented segmentation process provided more satisfactory solutions than the conventional methods.

Table 2. Recommended segmentation process's overall comparative examination for the first dataset over traditional optimization algorithms and segmentation techniques

Heuristic model-aided experiment					
Terms	RSO-OFCM [31]	DMO-OFCM [32]	OOA-OFCM [33]	HO-OFCM [26]	AHO-OFCM
"Coefficient of similarity"	0.855022862	0.761389397	0.784497528	0.804578814	0.897129496
"Spatial Overlap"	0.767367239	0.832268257	0.760019921	0.81170411	0.837051626
"PSNR"	50.99988024	45.09823642	52.96506801	48.10642571	53.95102786
"Accuracy"	86.659728	82.08082608	81.53165709	84.09830077	92.80744807
"MSE"	0.053850584	0.055125288	0.059459138	0.055102579	0.049273082
Segmentation techniques-aided experiment					
Terms	Active Contour [34]	Binary Thresholding [35]	KMC [36]	FCM [27]	AHO-OFCM
"Accuracy"					
"Coefficient of similarity"	0.729587297	0.779881034	0.707983431	0.814309227	0.897129496
"Spatial Overlap"	0.828504369	0.798913617	0.78506683	0.763969976	0.837051626

"PSNR"	51.45457126	52.68754008	51.10100759	46.55601633	53.95102786
"Accuracy"	89.34132541	86.21044934	84.48514235	91.42114514	92.80744807
"MSE"	0.059072555	0.057425964	0.054375044	0.058597892	0.049273082

Table 3. Recommended segmentation process's overall comparative examination for the second dataset over traditional optimization algorithms and segmentation techniques

Heuristic model-aided experiment					
Terms	RSO-OFCM [31]	DMO-OFCM [32]	OOA-OFCM [33]	HO-OFCM [26]	AHO-OFCM
"Coefficient of similarity"	0.823830337	0.735077335	0.775173148	0.8479553	0.861533926
"Spatial Overlap"	0.774590411	0.84382116	0.791780476	0.780964119	0.847293481
"PSNR"	50.01832107	49.19228873	54.6366247	48.32598291	54.72651029
"Accuracy"	84.62171815	81.35189289	81.48691709	90.24470325	92.39234549
"MSE"	0.056462147	0.04179992	0.055123023	0.042153562	0.040361703
Segmentation techniques-aided experiment					
Terms	Active Contour [34]	Binary Thresholding [35]	KMC [36]	FCM [27]	AHO-OFCM
"Coefficient of similarity"	0.777191157	0.777882683	0.737946567	0.844256212	0.861533926
"Spatial Overlap"	0.758586453	0.754696856	0.822423058	0.792545086	0.847293481
"PSNR"	52.51789396	54.57216399	52.00111445	45.0194784	54.72651029
"Accuracy"	90.39923857	86.58727453	84.42300592	80.78684652	92.39234549
"MSE"	0.055096121	0.055447056	0.054874022	0.04870632	0.040361703

6.7 Suggested LD prediction system's performance validation

The suggested LD prediction method's performance is examined for two datasets and employs the batch size values. Fig.13 depicts the LD prediction process's performance for the first dataset over classical techniques. Fig.14 illustrates the LD prediction process's performance for the second dataset over classical techniques. For the 32nd batch size in Fig.13 (b), the presented LD prediction task's F1-score is 31.25%, 18.75%, 3.75%, and 21.25% enriched than the classical techniques including Mobilenet, Shufflenet, CNN, and GCNN correspondingly. For the 16th batch size value in Fig.14 (c), the LD prediction task's FPR is 12%, 17%, 10%, and 3% decreased than the other techniques including Mobilenet, Shufflenet, CNN, and GCNN appropriately. Thus, it has been guaranteed that the developed prediction strategy of LD achieved high-quality outcomes than the existing techniques.

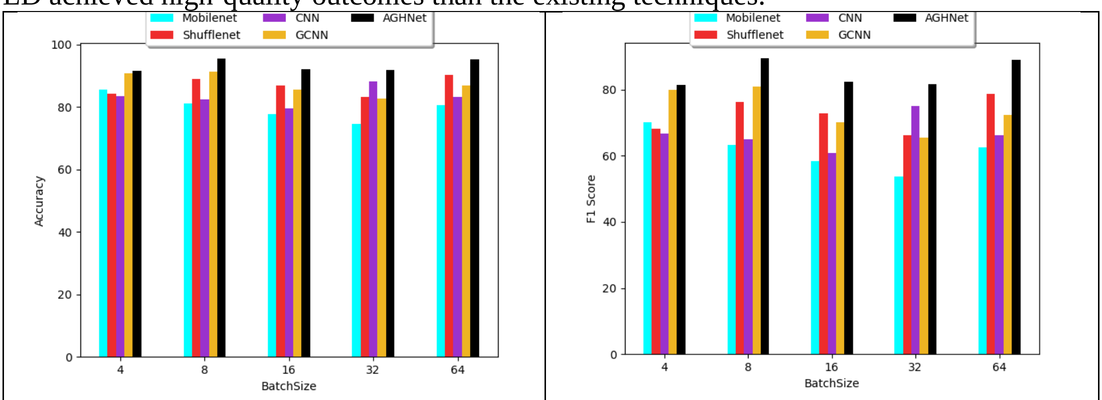

(a) (b)

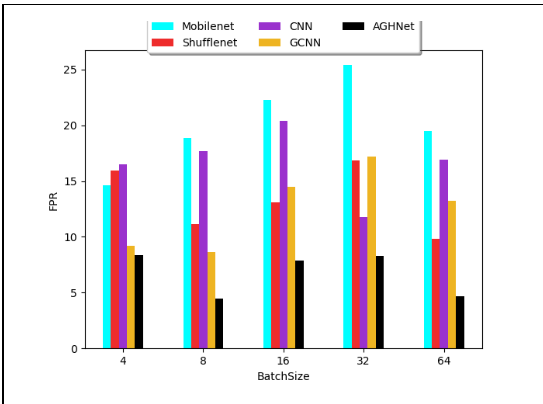

(c)

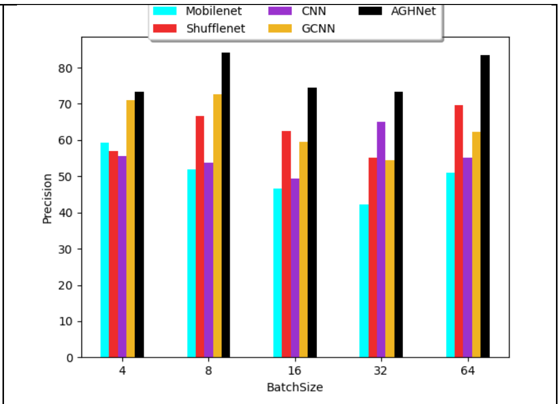

(d)

Fig. 13. Suggested LD prediction system's performance validation for the first dataset over traditional classifiers concerning " (a) Accuracy, (b) F1 score, (c) FPR, and (d) Precision"

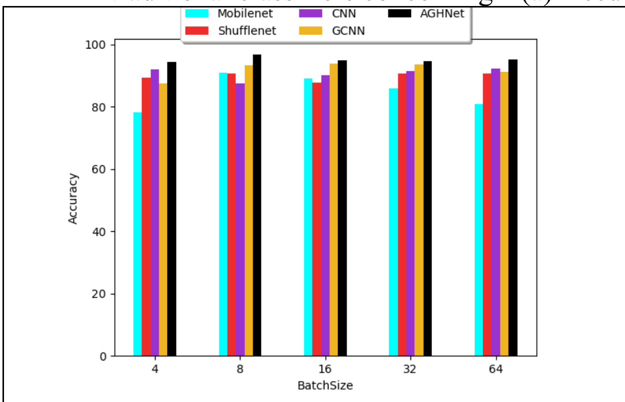

(a)

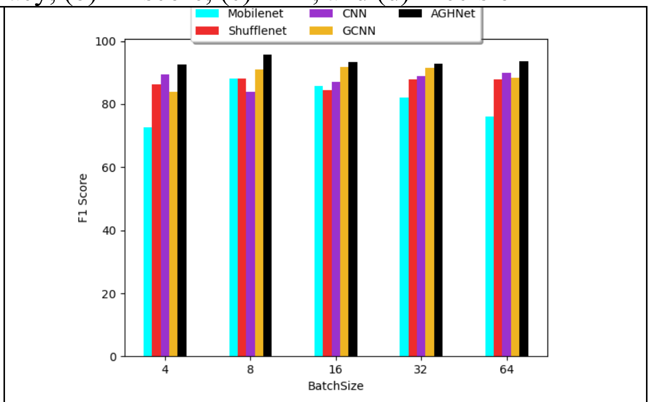

(b)

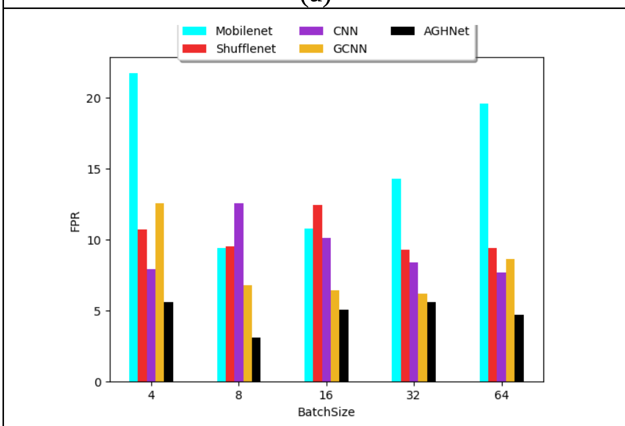

(c)

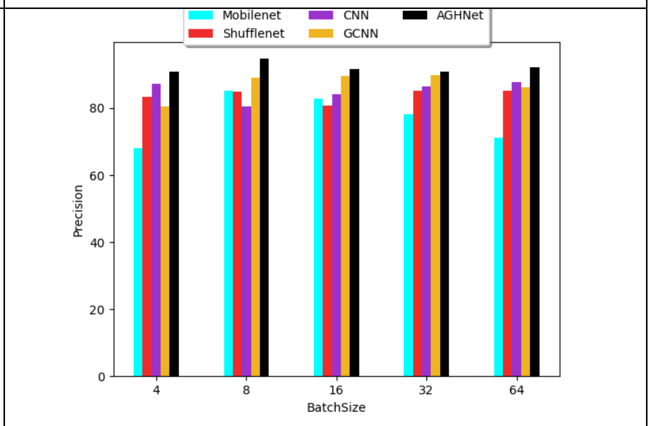

(d)

Fig. 14. Suggested LD prediction system's performance validation for the second dataset

over traditional classifiers concerning " (a) Accuracy, (b) F1 score, (c) FPR, and (d) Precision"

6.8 Suggested LD prediction system's overall comparative validation

The designed prediction system of LD is experimented by employing the 500th hidden neuron count and provided in Table 4 for two datasets. When considering the first dataset, the suggested LD prediction system achieved 8.8%, 13.6%, 7%, and 5.97% higher sensitivity than the existing models including Mobilenet, Shufflenet, CNN, and GCNN appropriately. When considering the second data source, the recommended LD prediction system's accuracy is 5.38%, 11.65%, 6.26%, and 2.09% improved than the conventional classifiers including Mobilenet, Shufflenet, CNN, and GCNN correspondingly. Therefore, it has been elucidated that the implemented LD prediction strategy obtained more satisfactory solutions than the existing techniques.

Table 4. Suggested LD prediction system's overall comparative validation for two datasets over traditional classifiers

Terms	Mobilenet [37]	Shufflenet [38]	CNN [39]	GCNN [28]	AGHNet
"Dataset 1"					
"Accuracy"	88.965517	84.200627	90.721003	91.724138	97.554859
"Sensitivity"	13.479624	14.733542	8.4639498	9.4043887	2.8213166
"FPR"	3.6256324	4.2039356	2.284264	2.4916944	0.7171315
"MK"	57.058465	40.95723	61.219421	65.919313	88.825373
"TS"	61.061947	51.908397	66.363636	68.646081	88.825215
"Dataset 2"					
"Accuracy"	91.618497	85.549133	90.751445	94.797688	96.820809
"Sensitivity"	9.7826087	12.318841	9.057971	5.0724638	2.5362319
"FPR"	28.421053	38.636364	28.409091	17.5	9.5890411
"MK"	96.346044	70.941307	87.286822	92.781955	92.820513
"TS"	89.568345	82.876712	88.69258	93.571429	96.071429

7. Conclusion

A novel LD prediction framework has presented in the model by incorporating deep learning. Initially, distinct benchmark sources were utilized for gathering significant images. Further, the garnered images were processed into the segmentation module, where the OFCM technique was taken for segmenting the irregularities that exist in the medical images. In this process, for improving accuracy and performance, the AHO was adopted. Further, the segmented images were given in the module for predicting the LD with the aid of AGHNet. Here, the GCNN, attention, and RNN models were combined for producing the highly accurate predicted outcomes. In the end, the experiments were performed for analyzing the designed process with various metrics. When considering the 64th batch size value in the second dataset, the accuracy of the designed LD prediction strategy was 17.89%, 5.26%, 3.15%, and 4.21% maximized than the existing classifiers such as Mobilenet, Shufflenet, CNN, and GCNN respectively. The experiments proved that the recommended LD prediction process made timely predictions with higher accuracy rates than the previous models. Though the implemented AGHNet-based LD prediction system is very effective and fast, the integration of GCNN and RNN may cause interpretability issues. In future work, this issue will be considered and rectified with the support of improved strategies.

References

1. Devikanniga, D., Ramu, A. and Haldorai, A., "Efficient diagnosis of liver disease using support vector machine optimized with crows search algorithm", EAI Endorsed Transactions on Energy Web, vol.7, pp.e10-e10, 2020.
2. Assegie, T.A., Subhashni, R., Kumar, N.K., Manivannan, J.P., Duraisamy, P. and Engidaye, M.F., "Random forest and support vector machine based hybrid liver disease detection", Bulletin of Electrical Engineering and Informatics, vol.11, pp.1650-1656, 2022.
3. Shah, R. and Solanki, P., "Recent Developments In Machine Learning Approach For Liver Disease Prediction", Journal of Namibian Studies: History Politics Culture, vol.35, pp.2278-2301, 2023.
4. Ahn, J.C., Connell, A., Simonetto, D.A., Hughes, C. and Shah, V.H., "Application of artificial intelligence for the diagnosis and treatment of liver diseases", Hepatology, vol.73, pp.2546-2563, 2021.
5. Raja, G., Reka, K., Murugesan, P. and Meenakshi Sundaram, S., "Predicting Liver Disorders Using an Extreme Learning Machine", SN Computer Science, vol.5, no.677, 2024.
6. Ramesh, V., "Predicting and Classifying Liver Functionality Disease through Machine Learning Methods", Journal For Innovative Development in Pharmaceutical and Technical Science (JIDPTS), vol.7, 2024.
7. Islam, M., Vasker, N. and Hasan, M., "Liver Disease Diagnostics with Explainable AI and Deep Learning", International Journal of Computing and Digital Systems, vol.16, pp.189-200, 2024.
8. Che, H., Brown, L.G., Foran, D.J., Nosher, J.L. and Hacihaliloglu, I., "Liver disease classification from ultrasound using multi-scale CNN", International Journal of Computer Assisted Radiology and Surgery, vol.16, pp.1537-1548, 2021.
9. Nakatsuka, T., Tateishi, R., Sato, M., Hashizume, N., Kamada, A., Nakano, H., Kabeya, Y., Yonezawa, S., Irie, R., Tsujikawa, H. and Sumida, Y., "Deep learning and digital pathology powers prediction of HCC development in steatotic liver disease", Hepatology, pp.10-1097, 2024.
10. Shaban, W.M., "Early diagnosis of liver disease using improved binary butterfly optimization and machine learning algorithms", Multimedia Tools and Applications, vol.83, pp.30867-30895, 2024.
11. Arslan, R.U., Pamuk, Z. and Kaya, C., "Usage of Weka Software Based on Machine Learning Algorithms for Prediction of Liver Fibrosis/Cirrhosis", Black Sea Journal of Engineering and Science, vol.7, pp.17-18, 2024.
12. Hendi, A.M., Hossain, M.A., Majrashi, N.A., Limkar, S., Elamin, B.M. and Rahman, M., "Adaptive Method for Exploring Deep Learning Techniques for Subtyping and Prediction of Liver Disease", Applied Sciences, vol.14, no.1488, 2024.
13. Veeranki, S.R. and Varshney, M., "Intelligent techniques and comparative performance analysis of liver disease prediction", International Journal of Mechanical Engineering, vol.7, pp.489-503, 2022.
14. Atabaki-Pasdar, N., Ohlsson, M., Viñuela, A., Frau, F., Pomares-Millan, H., Haid, M., Jones, A.G., Thomas, E.L., Koivula, R.W., Kurbasic, A. and Mutie, P.M., "Predicting and elucidating the etiology of fatty liver disease: A machine learning modeling and validation study in the IMI DIRECT cohorts", PLoS medicine, vol.17, no.e1003149, 2020.

15. Pei, X., Deng, Q., Liu, Z., Yan, X. and Sun, W., "Machine learning algorithms for predicting fatty liver disease", Annals of Nutrition and Metabolism, vol.77, pp.38-45, 2021.
16. Singh, J., Bagga, S. and Kaur, R., "Software-based prediction of liver disease with feature selection and classification techniques", Procedia Computer Science, vol.167, pp.1970-1980, 2020.
17. Fathi, M., Nemati, M., Mohammadi, S.M. and Abbasi-Kesbi, R., "A machine learning approach based on SVM for classification of liver diseases", Biomedical Engineering: Applications, Basis and Communications, vol.32, no.2050018, 2020.
18. Dai, R., Sun, M., Lu, M. and Deng, L., "Deep Learning for Predicting Fibrotic Progression Risk in Diabetic Individuals with Metabolic Dysfunction-associated Steatotic Liver Disease Initially Free of Hepatic Fibrosis", Heliyon, 2024.
19. Yao, Z., Li, J., Guan, Z., Ye, Y. and Chen, Y., "Liver disease screening based on densely connected deep neural networks", Neural Networks, vol.123, pp.299-304, 2020.
20. Afrin, S., Shamrat, F.J.M., Nibir, T.I., Muntasim, M.F., Moharram, M.S., Imran, M.M. and Abdulla, M., "Supervised machine learning based liver disease prediction approach with LASSO feature selection", Bulletin of Electrical Engineering and Informatics, vol.10, pp.3369-3376, 2021.
21. Wong, G.L.H., Yuen, P.C., Ma, A.J., Chan, A.W.H., Leung, H.H.W. and Wong, V.W.S., "Artificial intelligence in prediction of non-alcoholic fatty liver disease and fibrosis", Journal of gastroenterology and hepatology, vol.36, pp.543-550, 2021.
22. Dalal, S., Onyema, E.M., and Malik, A., "Hybrid XGBoost model with hyperparameter tuning for prediction of liver disease with better accuracy", World Journal of Gastroenterology, vol.28, no.6551, 2022.
23. Liu, Y., Meric, G., Havulinna, A.S., Teo, S.M., Ruuskanen, M., Sanders, J., Zhu, Q., Tripathi, A., Verspoor11, K., Cheng12, S. and Jain, M., "Early prediction of liver disease using conventional risk factors and gut microbiome-augmented gradient boosting", 2020.
24. Hashem, S., ElHefnawi, M., Habashy, S., El-Adawy, M., Esmat, G., Elakel, W., Abdelazziz, A.O., Nabeel, M.M., Abdelmaksoud, A.H., Elbaz, T.M. and Shousha, H.I., "Machine learning prediction models for diagnosing hepatocellular carcinoma with HCV-related chronic liver disease", Computer methods and programs in biomedicine, vol.196, no.105551, 2020.
25. Md, A.Q., Kulkarni, S., Joshua, C.J., Vaichole, T., Mohan, S., and Iwendi, C., "Enhanced preprocessing approach using ensemble machine learning algorithms for detecting liver disease", Biomedicines, vol.11, no.581, 2023.
26. Chowdhary, C.L., Mittal, M., P, K., Pattanaik, P.A. and Marszalek, Z., "An efficient segmentation and classification system in medical images using intuitionist possibilistic fuzzy C-mean clustering and fuzzy SVM algorithm", Sensors, vol.20, no.3903, 2020.
27. Djenouri, Y., Belhadi, A., Srivastava, G. and Lin, J.C.W., "Hybrid graph convolution neural network and branch-and-bound optimization for traffic flow forecasting", Future Generation Computer Systems, vol.139, pp.100-108, 2023.
28. Jun, K., Lee, D.W., Lee, K., Lee, S. and Kim, M.S., "Feature extraction using an RNN autoencoder for skeleton-based abnormal gait recognition", IEEE Access, vol.8, pp.19196-19207, 2020.
29. Zhang, B., Xiao, W., Xiao, X., Sangaiah, A.K., Zhang, W. and Zhang, J., "Ransomware classification using patch-based CNN and self-attention network on embedded N-grams of opcodes", Future Generation Computer Systems, vol.110, pp.708-720, 2020.
30. Dhiman, G., Garg, M., Nagar, A., Kumar, V. and Dehghani, M., "A novel algorithm for global optimization: rat swarm optimizer", Journal of Ambient Intelligence and Humanized Computing, vol.12, pp.8457-8482, 2021.
31. Agushaka, J.O., Ezugwu, A.E. and Abualigah, L., "Dwarf mongoose optimization algorithm", Computer methods in applied mechanics and engineering, vol.391, no.114570, 2022.

32. Dehghani, M. and Trojovský, P., "Osprey optimization algorithm: A new bio-inspired metaheuristic algorithm for solving engineering optimization problems", Frontiers in Mechanical Engineering, vol.8, no.1126450, 2023.
33. Mohammad Hussein Amiri, Nastaran Mehrabi Hashjin, Mohsen Montazeri, Seyedali Mirjalili and Nima Khodadadi, "Hippopotamus optimization algorithm: a novel nature-inspired optimization algorithm", Scientific Reports, Vol. 14, No. 5032, 2024.
34. Iqbal, E., Niaz, A., Memon, A.A., Asim, U. and Choi, K.N., "Saliency-driven active contour model for image segmentation", IEEE Access, vol.8, pp.208978-208991, 2020.
35. Gharehchopogh, F.S. and Ibrikci, T., "An improved African vultures optimization algorithm using different fitness functions for multi-level thresholding image segmentation", Multimedia Tools and Applications, vol.83, pp.16929-16975, 2024.
36. Khan, A.R., Khan, S., Harouni, M., Abbasi, R., Iqbal, S. and Mehmood, Z., "Brain tumor segmentation using K-means clustering and deep learning with synthetic data augmentation for classification", Microscopy Research and Technique, vol.84, pp.1389-1399, 2021.
37. Tekerek, A. and Al-Rawe, I.A.M., "A novel approach for prediction of lung disease using chest x-ray images based on DenseNet and MobileNet", Wireless Personal Communications, pp.1-15, 2023.
38. Ullah, N., Raza, A., Khan, J.A. and Khan, A.A., "An effective approach for automatic COVID-19 detection from multiple image sources using shufflenet convolutional neural network (CNN)", 2022.
39. Tyagi, A. and Mehra, R., "An optimized CNN based intelligent prognostics model for disease prediction and classification from Dermoscopy images", Multimedia Tools and Applications, vol.79, pp.26817-26835, 2020.